Tellus SERIES B CHEMICAL AND PHYSICAL METEOROLOGY
PUBLISHED BY THE INTERNATIONAL METEOROLOGICAL INSTITUTE IN STOCKHOLM

Tellus (2009), 61B, 473–482
Printed in Singapore. All rights reserved

TELLUS

On small particles in the Arctic summer boundary layer: observations at two different heights near Ny-Ålesund, Svalbard

By JOHAN STRÖM[1,2]*, ANN-CHRISTINE ENGVALL[3], FRANK DELBART[4], RADOVAN KREJCI[3] and RENATE TREFFEISEN[5], [1]*Department of Applied Environmental Science, Stockholm University, 106 91 Stockholm, Sweden;* [2]*Norwegian Polar Institute, 9296 Tromsø, Norway;* [3]*Norwegian Institute for Air Research (NILU), P.O. Box 100, N-2027 Kjeller, Norway;* [4]*CNRS, IPEV – French Polar Institute, 29280 Plouzané, France;* [5]*Alfred Wegener Institute, 14473 Potsdam, Germany*

(Manuscript received 15 May 2008; in final form 14 November 2008)

ABSTRACT

Concurrent observations of particle number densities and size distributions observed at two different heights (near ocean level and 475 m above sea level) in Ny-Ålesund, Svalbard were studied with respect to the diurnal variation during a summer period in June 2004. The results show that observed variation in particle number density in the Arctic boundary layer may be strongly modulated by vertical mixing and dilution. The particles appeared to be formed in the early morning when solar intensity reached about 30% of the mid-day intensity. Based on differences in the observed number densities at the two heights it appears as if particles are formed in the lower part of the boundary layer. The formation rate of 10 nm diameter particles is estimated to be 0.11 cm^{-3} s^{-1} and the growth rate is in a range between 1 and 2 nm h^{-1}.

1. Introduction

The key finding number one in the recent ACIA report (Hassol, 2005) states that during the past few decades the rate at which the Arctic has been warming is almost twice that of the global average. Retreating snow and ice cover, and changes in the extent of the permafrost caused by the warming are examples of feedback processes that may influence ocean circulations and the sources and sinks of greenhouse gases from soils.

The Arctic is not only responding to a changing climate, processes acting within the Arctic may impact other parts of the world as well. Aerosols and clouds are very important components in the Earth's energy budget, but among the least understood (IPCC, 2007). Rinke et al. (2004) studied the direct climate effect of aerosols using the Arctic regional atmospheric model HIRHAM. It was shown that the direct aerosol effect (scattering and absorption of sunlight) has the potential to change the mode and/or the strength of large-scale teleconnection patterns such as the Barents Sea Oscillation. These oscillations are associated with the inter-annual and decadal variability of Arctic climate processes and are connected with the climate of Europe.

To understand aerosol–cloud–climate interactions, we first have to understand the aerosol life cycle; formation, growth and transformation, transport and interaction with clouds. Precipitating clouds are essentially the only effective way of removing submicron particles from the atmosphere. The Arctic summer atmosphere is of particular interest as the atmosphere contains relatively few particles available to form cloud droplets. With a limitation in cloud-forming aerosols the cloud drops tend to be large and the clouds prone to form drizzle (Curry, 1995). The precipitating cloud in turn influences the aerosol population. Changes in the availability of cloud-forming aerosol particles may thus influence the hydrological cycle as well. Most of the aerosol particles observed in the Arctic, with respect to the number density, are formed there (Ström et al., 2003). Over a timescale of a few days these new particles may grow in size, making them potentially cloud-forming particles. Hence, an understanding of the processes controlling the aerosol population is imperative to understand Arctic clouds and climate.

In this study, we will investigate the temporal and spatial variations of small particles observed at different locations and different heights near Ny-Ålesund, Svalbard. We will focus on a two-week period in June 2004. Data will be analysed with

*Corresponding author.
e-mail: johan@itm.su.se
DOI: 10.1111/j.1600-0889.2008.00412.x

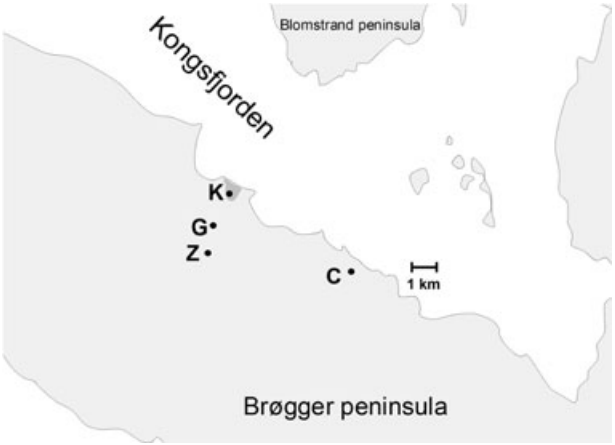

Fig. 1. Map over the Brøgger peninsula showing the location of the Zeppelin station (Z), Gruvbadet (G), Koldewey station (K) and the Corbel station (C). The research village Ny-Ålesund (78°55′N, 11°56′E) is indicated with a darker grey area where the Koldewey station is located.

respect to the observed diurnal variation of particle number densities and size distributions.

2. Sites and instrumentation

The locations where data used in this study were collected are indicated in Fig. 1. The Zeppelin station is located on the ridge of the Zeppelin Mountain about 2.3 km south of Ny-Ålesund. The station is situated at 474 m altitude and accessible via cable car. The Corbel station is located about 5 km southeast of Ny-Ålesund and about 0.5 km from the Kongsfjord shoreline. During summer, the Corbel station is accessible by foot or by boat. The distance between these two stations is about 5 km. The Koldewey station is located in Ny-Ålesund, about 0.5 km from the fjord. Gruvbadet, which is not a station but sometimes used to host scientific equipment, is located between the Koldewey and Zeppelin stations at an elevation which is below 100 m msl.

Data gathered from the Zeppelin station include the total particle number density and the aerosol size distribution. The particle number density (N_{10}) is measured using a condensation particle counter (CPC), model TSI 3010, with nominal 50% cut-off at 10 nm diameter (as indicated by the subscript). The size distribution is measured using a differential mobility particle sizer (DMPS), which scans size bins from 20 to 630 nm diameter with a resolution of $d\log D_p = 0.1$ (D_p is the particle diameter). A TSI 3010 CPC is used in this DMPS system. During the observation period, N_{10} data were stored every minute and a size distribution from the DMPS system was stored every second minute.

Observations performed by the Alfred Wegener Institute (AWI) are part of the international meteorological network. Data from the Corbel station include the total particle number density measured using the same type of CPC as at the Zeppelin station. Although instrumentation to measure atmospheric state and wind parameters are installed at all three stations, we have chosen to work with data from the Koldewey station as being representative of the conditions for the sampling area.

Besides the atmospheric state parameters and wind data observed at the Koldewey station, we also make use of radiosonde data. The data set includes daily meteorological launches at 11 UTC. Throughout the study UTC time will be used. Local time is UTC + 2 h in the summer period. Relative humidity (RH) data from routine launches must be corrected to account for systematic errors and time lag problems. We have corrected the data according to the procedure described in Treffeisen et al. (2007).

At Gruvbadet, a volatility tandem version of a DMPS (TDMPS) system was installed during the ASTAR 2004 experiment (http://www.awi.de/de), which coincided with the time period of this study. In a TDMPS, two DMPS systems are operated in series and the aerosol is conditioned (typically heated or humidified) after the first system and the modified aerosol is characterized by the second system. In this study, we will only use the data from the first system that essentially works as a normal DMPS. The drawback with the TDMPS system is that it takes longer time to scan over the size distribution. In our case, the system at Gruvbadet delivered one size distribution per hour for size bins between 5 and 300 nm diameter with a resolution of $d\log D_p = 0.1$. The CPCs used in this system were two TSI 3025 with a nominal cut-off at 3 nm diameter. The inversion of the data considers particle charge probability and ideal transfer function, but neither the CPC cut-off characteristics nor diffusion losses are included in the calculations. While this introduces an uncertainty in quantifying the smallest particles, the data will be used in a semi-qualitative way (studying the evolution of the shape of the distribution rather than absolute number densities) and thus should be a minor problem. Unfortunately, a problem in the data logging software of the system in Gruvbadet caused the loss of data during the first 2 h of each day.

3. Observations

Based on observations from the Zeppelin station, Ström et al. (2003) showed that the shape of the Arctic aerosol size distribution undergoes a rapid transition between spring and summer. From being dominated by an accumulation mode in spring, the distribution shifts to being dominated by an Aitken mode in summer. From a compilation of 6 yr of data, Engvall et al. (2008) showed that this feature repeats itself from year-to-year within a time window of approximately two weeks. The authors proposed a criterion, based on the observed aerosol condensational sink and solar radiation, to determine if summer conditions were met. For the year 2004, this criterion suggests that the transition took place around day-of-year 145 (24 May).

Figure 2 shows a time-series of N_{10} observed at the Zeppelin station from 10 May to 17 June 2004 which is a period covering about two weeks before and three weeks after this transition

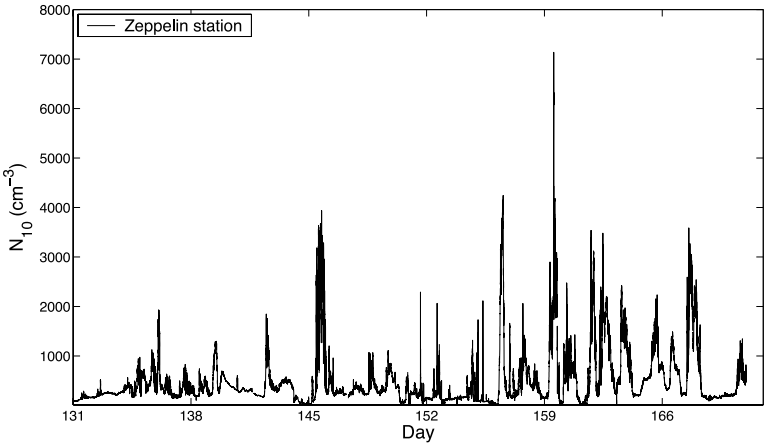

Fig. 2. Particle number density (diameter larger than 10 nm) observed at the Zeppelin station from 10 May to 18 June 2004.

date. Besides a peek up to about 4000 cm^{-3} near the date of transition, there is no obvious difference in the particle number density right before and after 24 May 2004. However, from about day-of-year 156 (4 June) N_{10} frequently exceeds 2000 cm^{-3} with a periodic appearance.

We were very intrigued by this pattern and selected this two week summer period, between 4 and 17 June 2004 for our comparison of N_{10} measured at the Zeppelin station and at the Corbel station.

3.1. *Comparison between Corbel and Zeppelin particle number density time-series*

Figure 3 presents the hourly averaged N_{10} observed at the Zeppelin and Corbel stations for the selected two week period. Data range over two orders of magnitude from a few tens to several thousand particles per cubic centimetre. The variations in N_{10} are episodic and characterized by oscillations, causing some 10–12 periods with rather distinct increases and decreases in the number density. Despite the distance of almost 500 m in the vertical and 5 km in the horizontal direction, the two data sets follow each other very closely over this time period.

The correlation (r^2) between the two time-series is about 0.7, using minute averages of log(N_{10}). The use of the logarithm is to give high and low number densities similar weights over the time-series. By shifting the data in relation to each other and recalculating the correlation after each minute shifted, it is possible to study any systematic time lag between the data sets. The result is presented in Fig. 4, where negative shifted minutes mean that Zeppelin data trail the Corbel data. A slight improvement in the correlation could be achieved by shifting the Zeppelin data back in time a few minutes, meaning the Zeppelin data would lag the Corbel data by a few minutes. The correlation drops below 0.5 when the data sets are shifted more than 150–200 min. The time stamp at the Zeppelin station is based on internet time, whereas the data logging at the Corbel station is based on a PC clock. Clocks in PCs are known to be notoriously inaccurate, but the PC at Corbel had recently been manually adjusted to correct UTC time. Hence, if the times at the two stations differ, it should be by only a few minutes.

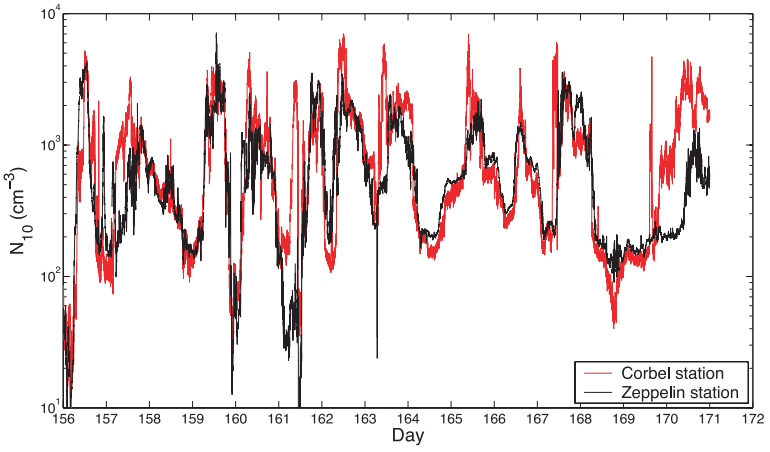

Fig. 3. Particle number density (diameter larger than 10 nm) observed at the Zeppelin and Corbel stations between 4 and 18 of June 2004.

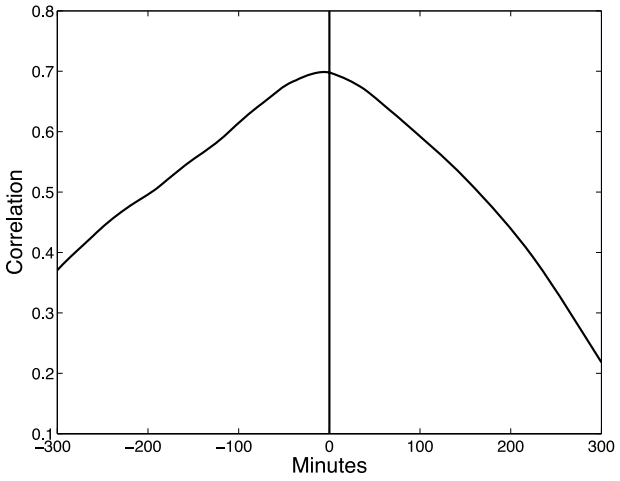

Fig. 4. Correlation (r^2) between particle number density observed at the Zeppelin and Corbel stations after shifting the two data sets in relation to each other. Negative time-shift corresponds to Zeppelin data leading Corbel data and vice versa.

The fact that the maximum correlation occurs close to the zero time-shift has important implications. The reason is that the characteristic time it would take an air parcel to travel between the two stations is many times longer than a few minutes. The maximum 1 h averaged wind speed observed at the Koldewey station was less than 10 m s^{-1} with a median value of about 2.5 m s^{-1}. The median wind speed corresponds to a traveltime of approximately half an hour. This assumes a transport from C to Z (cf. Fig. 1) or vice versa.

In Ny-Ålesund, the wind direction often follows the fjord which is evident from the histogram presented in Fig. 5. As the air is approaching the stations from essentially two directions, alternating time lag between the data sets might cause them to cancel each other when calculating correlation on the entire data set. To test this, we divided the data into two sets with wind from the east (wind directions between 0° and 180°) or west (wind directions between 180° and 360°). The correlation calculations were repeated for each of the two groups of data. The splitting of the data improved the maximum correlation slightly (0.74 for wind from east and 0.72 for wind from west) but did not indicate any systematic time lag between the two stations (not shown).

Hence, variations in the N_{10} time-series between the stations do not typically lag by any more than a few minutes. This analysis suggests that observed changes in particle number density are not primarily variations in the lateral direction. If this were the case, there should be a clear separation in time between features observed at the two stations. Depending on the wind direction, one or the other station would detect a change in N_{10} before the other. That is, when air moves into the fjord changes in N_{10} would first be observed at the Zeppelin station and after typically 20 min to 1 h later the same change would be observed at the Corbel station and vice versa.

3.2. *Diurnal variations in particle number density at the Zeppelin and Corbel stations*

The visual impression of the time-series in Fig. 3 suggests that oscillations between high and low values occur within a period of about 1 d. This is confirmed by a Fourier analysis performed on the two data sets and presented in Fig. 6. As expected, the 1 d period shows up very clearly in the spectra. In addition to the 1 d period, the 1.5, 2 and 3 d periods are also evident in the spectra, but with smaller amplitudes. Encouraged by the results of the Fourier analysis, we explored the diurnal variations further by grouping the data by the hour of the day and make averages for each hour. With these averages we compiled an average-day for

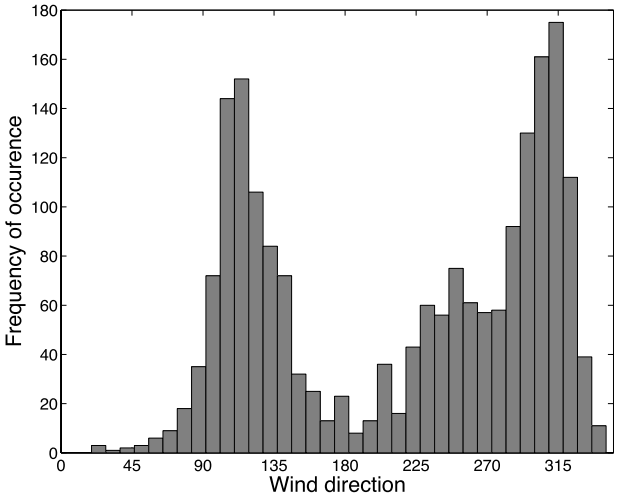

Fig. 5. Frequency distribution of 10 min averaged wind direction observed at the Koldewey station between 4 June and 18 June 2004.

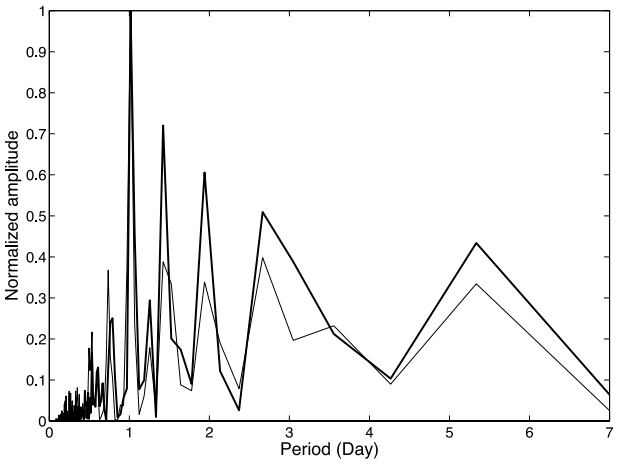

Fig. 6. Normalized amplitude as function of period from Fourier analysis of the N_{10} time-series, where thick line is Zeppelin data and the thin line is Corbel data.

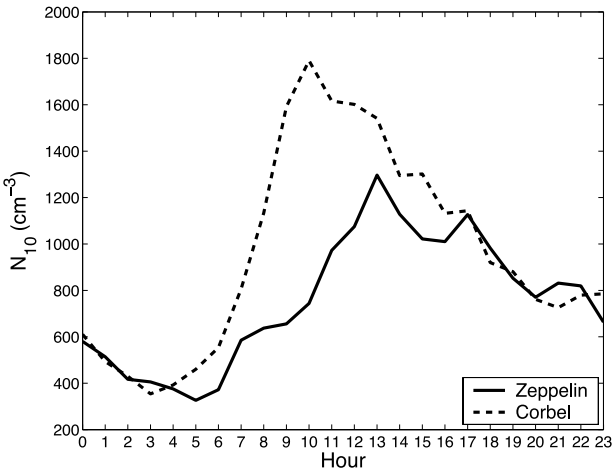

Fig. 7. Particle number density averaged for each hour of the day between 4 and 18 June 2004. Solid line is data from the Zeppelin station. Dashed line is data from the Corbel station.

each of the two data sets (Corbel and Zeppelin). The result is presented in Fig. 7.

At the start of the day both stations show about the same number density which decreases over the first hours of the day. Between 0300 and 0400 UTC in the morning the number density at Corbel reaches its minimum value. The minimum at the Zeppelin occurs about 2 h later between 0500 and 0600 UTC in the morning. Between 1000 and 1100 UTC the maximum number density is reached at the Corbel station. The maximum at the Zeppelin occurs about 3 h later between 1300 and 1400 UTC. The maximum at the Corbel station is almost 40% higher than the Zeppelin maximum number density. In the afternoon after about 1600 UTC, the two data sets merge again and follow each other for the remainder of the day and into the next day.

3.3. *Diurnal variations in the size distributions at the Zeppelin station and Gruvbadet*

Analogous to the average-day compiled for the CPC data, the size distributions were grouped by the hour of the day and the average distribution for each hour was calculated. The particle number density changes a lot over the course of a day. To follow the evolution of the distribution better, the distributions were normalized to the maximum dN/dlog D_p for each hour-averaged distribution (note that the first hours of the day at Gruvbadet are missing due to software problems). The normalized size distributions based on data from the two weeks investigation period are presented in Figs. 8a and b.

Both data sets show rather well-defined features, but their evolutions differ in appearance. Data from Gruvbadet shows a cyclic growth behaviour where 5 nm particles appear in the morning around 0500 UTC. The particles grow through the rest of the day and into the next day. The particles reach sizes around 30–40 nm diameter after 1 d of growth. On the other hand, data from the Zeppelin station show essentially one of two situations. Approximately, half of the time the Aitken mode and accumulation mode are comparable in magnitude, the other half of the time the Aitken mode dominates the distribution. Between 0200 and 1300 UTC the distribution presents a bimodal structure with an Aitken mode between 30 and 40 nm and an accumulation mode around 100 nm in diameter. After 1300 UTC until 0200 UTC the next day the accumulation mode is only suggested and the Aitken mode dominates. In the afternoon, the Aitken mode

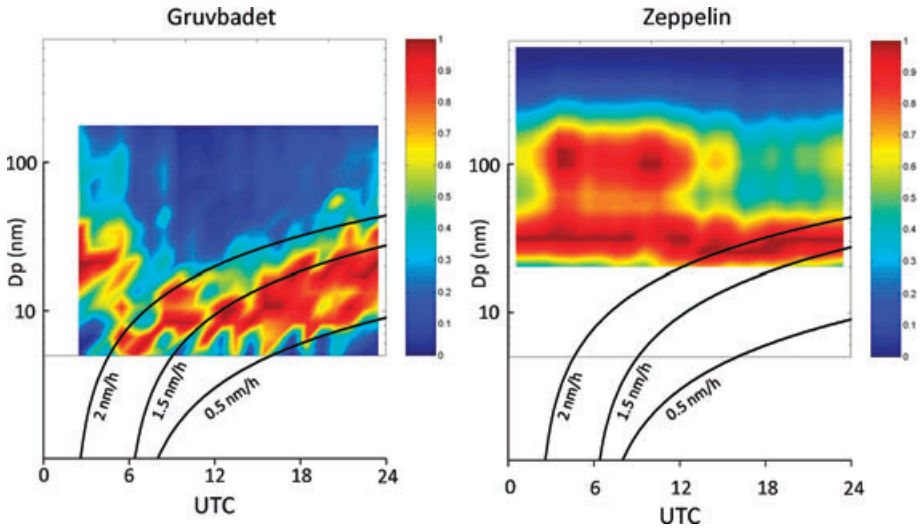

Fig. 8. Average day size distributions observed at Gruvbadet (left-hand side) and the Zeppelin station (right-hand side). The distributions are normalized to the maximum value each hour to follow the evolution of the shape of the distribution. The lines in the figures represent the evolution of different growth rates as indicated in the figure. Note that, since the Gruvbadet and the Zeppelin distributions do not cover the same size range a direct comparison of the normalized colour scales between the two data sets cannot be done.

initially drops below 30 nm diameter, but by 2000 UTC the mode is back between 30 and 40 nm.

For newly formed particles to be able to reach sizes around 30–40 nm diameter in 1 d, growth rates need to be between 1 and 2 nm h^{-1}. Particles formed early in the day are likely to have a faster growth rate than particles formed towards the end of the time window when new particles are formed. There are several arguments for this if one assumes that particle formation only occurs during a limited period of the day. New particle formation from gas-to-particle conversion is initiated when vapours reach a critical level and ceases once the condensational sink grows larger than the rate of supply, which brings the vapours below the critical level (Kulmala et al., 2001). Particles formed in the beginning of a formation event will likely have more excess vapour available for growth by condensation than particles forming towards the end when there are more particles to share the vapours. Growth by coagulation is a strong function of particle number density. Once the formation event is over and the supply of small particles drops, the growth rate by coagulation will decrease as well.

In Fig. 8, we have superimposed lines representing three different growth rates (2, 1.5 and 0.5 nm h^{-1}). The line representing 2 nm h^{-1} was adjusted to approximately follow the leading edge of the growing particles as observed at Gruvbadet. The line representing 0.5 nm h^{-1} was adjusted to approximately follow the trailing edge of the growing particles. The line 1.5 nm h^{-1} was adjusted to be somewhere in the middle of the growing particles. This graphical estimates suggest that particles may form very early in the day between around 0300 and 0800 UTC. Due to the high solar elevation during the Arctic summer, one-third of the mid-day solar intensity is already reached at around 0300 UTC, and by 0800 UTC almost 90% of the mid-day intensity is reached. The same growth rate lines attuned to data from Gruvbadet are also superimposed on data from the Zeppelin station. The appearance of 20 nm particles around noon at the Zeppelin station fits well with the growth of the earliest formed and fastest growing particles.

3.4. *Phenomenological interpretation of the diurnal variation*

The rapid increase of particles in the morning and the evolution of the size distribution observed at Gruvbadet are consistent with a cyclic formation of new particles through gas-to-particle conversion. However, the decrease in the afternoon is faster than can be explained by coagulation or dry deposition. Cloud scavenging could remove particles quickly, and a systematic occurrence of clouds could explain the observed diurnal variation in particle number density. As clouds were essentially above all three stations during the measurement period, we exclude this process as responsible to the observed variations. The only conceivable process that could reduce N_{10} with the observed rate is dilution. To get an idea of the magnitude of dilution that could explain the observations, we will explore the diurnal cycle further by constructing a simple phenomenological model.

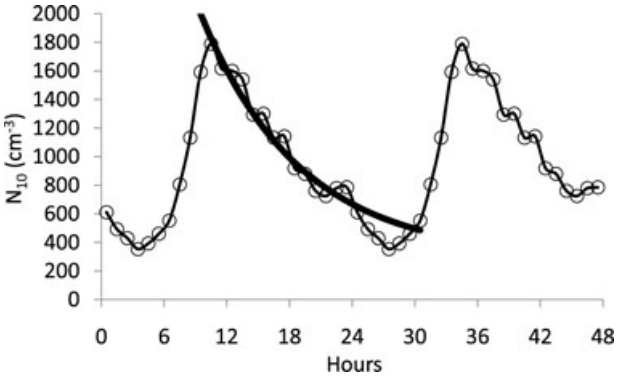

Fig. 9. Thin line with circles shows the hourly averaged particle number density data from Corbel as in Fig. 7 but presented as cyclic time-series for 2 d. Thick black line without symbols is the resulting number density if an initial value of 1800 cm^{-3} at 1000 is diluted 10% per hour with air of constant number density of 300 cm^{-3}.

We imagine two reservoirs, one representing the air observed at the Corbel station and the other representing a constant number density. Vertical distributions of N_{10} from aircraft measurements presented by Engvall et al. (2008), their Fig. 3, show a very stable number density of about 300 cm^{-3} just above the boundary layer (BL). We adopt this value for our constant number density. As shown in Fig. 9, an air parcel with initially 1800 cm^{-3} at 1000 UTC will fit the observed decrease rather well, if the air is diluted at a rate of about 10% per hour. That is to say, every hour 9/10 of the original number density is mixed with 1/10 of the constant number density.

To emulate the observed increase in N_{10}, we introduce a constant source of 400 cm^{-3} (10 nm particles) each hour between 0700 and 1100 UTC. The starting time for the source is suggested by the data from Gruvbadet (Fig. 8) where particles formed 0300 UTC and with a growth rate of 2 nm h^{-1} will reach a diameter of 10 nm between 0700 and 0800 UTC. Combining the simple source and dilution closely mimics the observed data as shown in Fig. 10a for an initial N_{10} at 0000 UTC of 550 cm^{-3}.

The Zeppelin station is located between the surface layer and the free troposphere. Analogous to the two reservoir approach for Corbel, we can view the situation for Zeppelin as three reservoirs, the lower level represented by Corbel, the upper level represented by the free troposphere and the Zeppelin level in between. If we assume the same initial N_{10} and mixing rate from the free troposphere as for Corbel, we can reproduce the diurnal variation at the Zeppelin station if we use a mixing rate of 30% per hour between the lower layer and the level at Zeppelin. That is to say, at hour 0100 the number density at the Zeppelin station is given by 60% from the previous hour (0000) at the same level, 30% from the previous hour at the level below and 10% from the free troposphere. As can be seen from the results presented

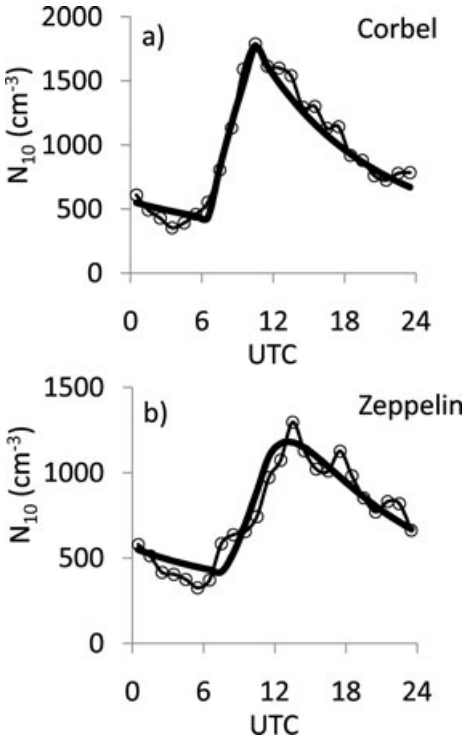

Fig. 10. The thin lines with open symbols are the observations as in Fig. 7. The thicker lines without symbols are the results from a simple phenomenological model, see text for details.

in Fig. 10b, the calculated N_{10} fits the observations well both in magnitude and timing.

This simplified model is not a simulation, but the fact that this idealized framework is able to capture the diurnal variation at two measurement sites, suggests that mixing and dilution is a very important process. The practical implication of theses mixing rates is that the 10% exchange rate will replenish more than 90% of the air in the BL in 1 d, and the 30% exchange rate will cause a 50% mixing in 3 h.

Hence, our interpretation of the data is as follows. The lack of time lag between the Corbel and the Zeppelin stations, based on the correlation study, indicates that processes controlling the evolution of N_{10} are not mainly related to variations in the lateral direction. Particles are formed in the lowest levels of the BL, at least below the Zeppelin station, since the increase in N_{10} is first observed at the Corbel station and the peak number densities is higher near the surface. The formation of new particles begins in the early hours of the day and continues throughout the morning. When the source of 10 nm particles stops, the dilution effect takes over and N_{10} decreases until the next day when the source of new particles begins again. The N_{10} evolution at the Zeppelin station is governed by the mixing of air from below and above the station. The number density at Corbel will begin to decrease earlier than at Zeppelin. This is due to the fact that as long as N_{10} at Corbel is higher than at Zeppelin, N_{10} at Zeppelin will continue to increase. In the afternoon when N_{10} at Corbel decreases to similar values as at Zeppelin, the two stations will follow each other until the next morning.

3.5. *The relation between horizontal wind, N_{10} and the vertical structure of the boundary layer*

In the simple model frame above, constant mixing rates were used. It is likely that these rates vary from day-to-day and even during the day. Mixing and turbulence are often linked to wind speed, where higher wind speeds are associated with increased turbulence and mixing. Periods with higher wind speed will then tend to show lower N_{10} due to stronger mixing. Figure 11 shows how N_{10} at Zeppelin and Corbel depends on the wind speed observed at the Koldewey station. Indeed, there is a clear relation, with N_{10} decreasing as the wind speed increases. At wind speeds above 6 m s^{-1} N_{10} do not exceed 2000 cm^{-3} at either station. Although, the highest number densities are observed during wind conditions below 3–4 m s^{-1}, the whole range of number densities is present at low wind speeds. Hence, for the period investigated in this study, low wind is a requirement but not a sufficient condition to observe high particle number densities. The relation between wind speed and N_{10} may not just be related to dilution. It is conceivable that wind conditions may be relevant to the formation process as well. Low wind speeds might favour the accumulation of precursor gases and the RH in the BL.

The link between mixing and wind speed can be illustrated by the RH and horizontal wind profiles observed by the daily radiosondes launched from Ny-Ålesund. An average wind speed between mid-night and 1200 UTC was calculated for each day based on the observed surface wind at Koldewey. The profiles were divided into two groups above and below the median wind speed. The median value was used to divide the data in two groups with equal number of profiles. For each of the two groups of RH profiles, the averages and standard deviations (*SD*s) were calculated over 50 m moving altitude levels. The ± 1 *SD* from the average RH are plotted for the two groups in Fig. 12a, and an analogous plot for the wind speed in Fig. 12b. Unfortunately, the wind data on 6 June 2004 was erroneous and thus not included in this analysis. Hence, for RH data there are seven profiles in each group above and below the median surface wind, whereas the wind data consist of six and seven profiles for below and above median wind, respectively. The upper RH ranges ($+1$ *SD*) are rather similar for the two data sets. Here, RH increases from around 80% near the surface to almost 100% just below 1.5 km. Above 1.5 km, RH decreases again and typically ranges between 80% and 90%. The mean temperature profile (not shown) presents a stable layer between about 1 and 2 km altitude, which places the mean inversion at about 1.5 km altitude. In the case of the lower ranges (minus one *SD*), the two RH data sets present a more systematic difference. This is, in particular, evident in the lowest kilometre, where the difference is more than 15 RH units

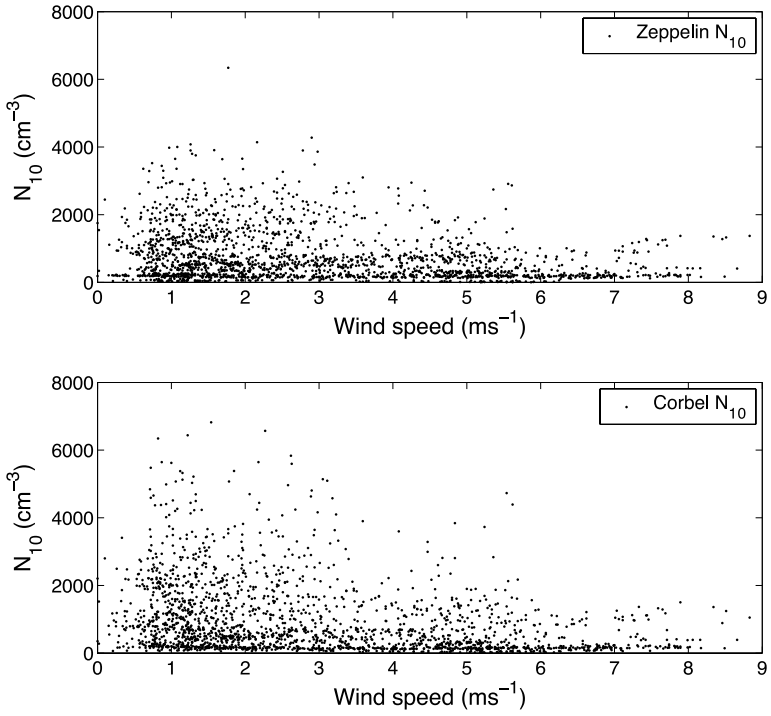

Fig. 11. Hourly averaged particle number density as function of hourly averaged wind velocities, Corbel data (bottom) and Zeppelin data (top).

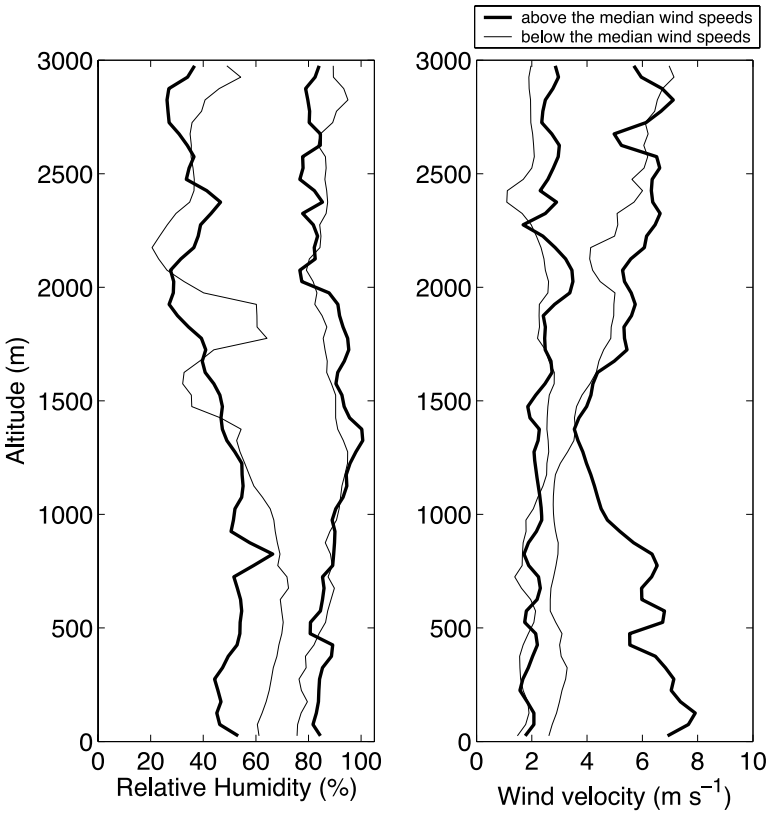

Fig. 12. Observations from routine radiosonde launches at the Koldewey station in NY-Ålesund. The range (±1 SD around the mean value) in observed relative humidity (a), and horizontal wind velocity (b). Thin lines represent periods when the surface winds were below the median wind speed based on averages between 0000 and 1200 UTC. Thick lines represent surface winds above the median value. See text for more details. Each RH range is based on seven profiles each. Due to error in radiosonde wind data on 6 June 2004, there are seven profiles for periods above median winds speed and six profiles for the below median wind speed.

for much of that altitude range. This dryer air in the lowest level suggests a stronger influence from the free troposphere when the observed mean wind is higher (i.e. stronger mixing). This is corroborated by the wind profiles in Fig. 12b. Below about 1 km altitude there is a systematic difference between the two data sets. The 'low' surface wind profiles maintain low speeds in a narrow range up to about 1 km altitude. Above this altitude the winds increase slightly while the range more or less gradually increases. The 'high' surface wind profiles are systematically higher in the lowest kilometre, but also characterized by a larger range. Above about 1 km the two data sets are more similar. Based on these profiles stronger winds appear to make the lowest kilometre dryer, which would suggest a larger influence from the free troposphere due to entrainment and mixing.

4. Discussion

We can compare our findings with that of Komppula et al. (2003) for Pallas (northern Finland) located 10° to the south at about 68°N. The authors analysed a more extensive data set comprising 2 yr of observations from two stations about 6 km apart and at 340 and 560 m altitudes, respectively. The constant particle formation rate used in our phenomenological explanation corresponds to a formation rate of 0.11 cm^{-3} s^{-1} for 10 nm particles, which compare well with their median value of 0.13 (range from 0.06 to 0.4 cm^{-3} s^{-1}) for 7 nm particles.

Growth rates observed at Pallas ranged between 1.4 and 8.2 nm h^{-1} (median value was 4 nm h^{-1}), which is faster growth than our estimate between 1 and 2 nm h^{-1}. It is likely that this simply reflects the more remote location of Svalbard compared to northern Finland. There is simply less material to build particles from. Starting times of 1 nm particle formation in Pallas were typically 0600–0700 UTC (range from 0250 to 1220 UTC (local time is UTC + 2 h), which means typically a few hours later than our estimate for Svalbard. Most of the formation events in Pallas occurred in spring and our data were from June. There is a large difference in solar elevation angles between these two places when comparing location and time of year, which probably explains the early formation at Svalbard. In case of the observations at Pallas, solar radiation was attributed a key factor needed to initiate particle formation.

By comparing the timing of the formation events at the two Finish stations, Komppula et al. (2003) concluded that vertical motion of air was more important than lateral advection. Vertical mixing processes between the BL and the free troposphere were also suggested by Wiedensohler et al. (1996) as a candidate to better explain occurrence of small particles in the Arctic during The International Arctic Ocean Expedition (IAOE-91) (1991). On the other hand Leck and Bigg (1999) argued that the lack of mixing in the Arctic summer atmosphere excluded a tropospheric source to form new particles. They proposed that bubble bursting on open leads provided material for both nucleation and larger particle formation.

The similarities, with respect to the diurnal development of small particles, between Pallas and Ny-Ålesund suggest that solar radiation and vertical mixing are important processes in shaping the temporal evolution of the aerosol. Given the appropriate reactive precursors, solar radiation will trigger the formation of condensable vapours that ultimately will nucleate particles provided that the preexisting condensational sink is sufficiently small. Dilution will lower the condensational sink and set the stage for subsequent formation events on a following day. Whether the mixing also introduces additional precursor gases from above or if the source is natural processes in the oceans is still to be determined.

The islands that are part of Svalbard are an obstacle for air motion and as could be the case for northern Finland, it is likely that the mountains influence the airflow as well. The fact that the growth of newly formed particles can be followed throughout the day tells us that the formation is not only a local phenomenon, but must take place on a much larger scale. Transport with the median wind for 1 d is equivalent to more than 200 km. This distance is about the scale of the width of Svalbard itself. Hence, air transported from east to west would have been at the eastern coastline 1 d prior to arriving Ny-Ålesund. Air transported from west to east would have been over the ocean one-third the distance to Greenland 1-d prior to arriving Ny-Ålesund. When air approaches from the west at least, the effect of Svalbard topography should be limited.

5. Conclusions

The main conclusion from this study is that the observed variation in particle number density in the Arctic BL during the summer period presented here is strongly modulated by mixing and dilution. The details about particle formation are still incomplete, but the diurnal appearance of small particles in the early hours of the day points towards photochemical chemistry as being the parameter for the source of precursor gases. The particles appear to be formed in the lowest layers, at least during the period investigated in this study. However, the large mixing makes the source identification difficult as important precursors may come from the surface layer as well as the free troposphere. As a matter of fact, much of the observed aerosol dynamics appears not so very different from that which has been reported in studies of aerosol evolution observed at lower latitudes (Kulmala et al., 2005).

6. Acknowledgments

This study was sponsored by the Swedish Environmental Protection Agency and the Swedish Research Council. Thanks to the staff of the Norwegian Polar Institute for helping with the equipment at the Zeppelin station and the French Polar

Institute/Arctic dept. for help with equipment at the Corbel station. The authors would also like to thank Birgitta Noone and Juri Waher for invaluable help with collecting the data.

References

Curry, J. 1995. Interactions among aerosols, clouds, and climate of the Arctic Ocean. *Sci. Tot. Environ.* **160/161**, 777–791.

Engvall, A. C., Krejci, R., Ström, J., Treffeisen, R., Scheele, R. and co-authors. 2008. Changes in aerosol properties during spring-summer period in the Arctic troposphere. *Atmos. Chem. Phys.* **8**, 445–462.

Hassol, S. J. 2005. *ACIA, Impacts of a Warming Arctic; Arctic Climate Impact Assessment*. Cambridge University Press, Cambridge.

IPCC 2007. Intergovernmental Panel on Climate Change (2007a), *Climate Change 2007—the Fourth Assessment Report of the IPCC*. Cambridge: Cambridge University Press, ISBN 978 0521 88009-1.

Leck, C. and Bigg, E. K. 1999. Aerosol production over remote marine areas—a new route. *Geophys. Res. Lett.* **26**, 3577–3580.

Komppula, M, Lihavainen, H., Hatakka, J. and Paatero, J. 2003. Observations of new particle formation and size distributions at two different heights and surroundings in subarctic area in northern Finland. *J. Geophys. Res.* **108**, 4295, doi:10.1029/2002JD002939.

Kulmala, M., Dal Maso, J., Mäkelä, L., Pirjola, M., Väkevä, P and co-authors. 2001. On the formation, growth and composition of nucleation mode particles. *Tellus* **53B**, 479–490.

Kulmala, M., Petäjä, T., Mömkkönen, P., Koponen, I. K., Dal Maso, M. and co-authors. 2005. On the growth of nucleation mode particles: source rates of condensable vapor in polluted and clean environments. *J. Atmos. Chem. Phys.* **5**, 409–416.

Rinke, A., Dethloff K. and Fortman M. 2004. Regional climate effects of Arctic haze. *Geophys. Res. Lett.* **31**, L16202, doi:10.1029/2004GL020318.

Ström, J., Umegård, J., Tørseth, K., Tunved, P., Hansson, H.-C. and co-authors. 2003. One year of particle size distribution and aerosol chemical composition measurements at the Zeppelin Station, Svalbard, March 2000-March 2001. *Phys. Chem. Earth* **28**, 1181–1190.

Treffeisen, R., Krejci, R., Ström, J., Engvall, A. C., Herber, A. and co-authors. 2007. Humidity observations in the Arctic troposphere over Ny-Ålesund, Svalbard based on 15 years of radiosonde data. *Atmos. Chem. Phys.* **7**, 2721–2732.

Wiedensohler, A., Covert, D. S., Swietlicki, E., Aalto, P., Heintzenberg, J. and co-authors. 1996. Occurrence of an ultrafine particle mode less than 20 nm in diameter in the marine boundary layer during Arctic summer and autumn. *Tellus* **48B**, 213–222.